Analysis of Vacancy defects in Hybrid Graphene-Boron Nitride Armchair Nanoribbon based n-MOSFET at Ballistic Limit

Anuja Chanana†, Amretashis Sengupta*, and Santanu Mahapatra†
†Department of Electronics Systems Engineering, Indian Institute of Science, Bangalore-560012, India
*School of VLSI Technology, Indian Institute of Engineering Science and Technology,
Shibpur, Howrah-711103, India
e-mail: anuja@cedt.iisc.ernet.in

Abstract

Here, we report the performance of hybrid Graphene-Boron Nitride armchair nanoribbon (a-GNR-BN) n-MOSFET at its ballistic limit using Non Equilibrium Green's Function (NEGF) methodology with different vacancy defects. The band gap and effective mass show a decrease which affects the device parameters showing an increase in ON-current (I_{ON}) and Sub Threshold Slope (SS).

Introduction

Embedding Graphene with Boron Nitride (nearly same lattice constant with graphene) is one of the effective ways of opening a band gap in gapless graphene and such atomic layers are synthesized experimentally [1].Ballistic device performance of a-GNR-BN based n-MOSFET and effect of Stone Wales(SW) defects using NEGF formalism is earlier investigated [2].Here, we analyze the performance of a-GNR-BN with vacancy defects monovacancy(single B atom removal), divacancy(one B and one N atom removal) and ring vacancy(removal of 2 B, 2 N and 2 C atoms) formed at the interface of graphene and BN nanoribbon.The defects are distributed randomly at the Graphene-Boron Nitride interface and are likely to be formed here [3].

Simulation Technique

We examine a super cell formed by repeating the 3p configuration of hybrid a-GNR-BN consisting of 30GNR atoms and 12BN atoms(6 on either side). The supercell of hybrid a-GNR-BN with 3 ring defects is shown in Fig1(a) with rest of the defects separately in Fig1(b)-(d).The bandgap and effective mass are calculated using DFT-LDA simulations on Quantumwise ATK [4]. Monkhorst-Pack k-grid mesh of 1x1x15 is used for the simulations.Further they are used in our in-house ballistic NEGF simulator [2] to evaluate the device characteristics. The channel length is 10 nm(Fig 1(e)),hence the transport is assumed to be purely ballistic.

Discussion

The band structure(Fig2(a)) for ring defect shows a larger decease as compared to mono and di vacancy defects confirmed by Density of States in Fig2(b). The band gap and effective mass values show a decrease with an increase in number of defects shown in Fig 2(c)-(d) and the decrement is largest for ring vacancy defect. For number of defects 3, I_{ON} from pure to defected device varies in the range of 276-293 μA (Fig 3(a)-(b)). For a ring defect density of 6.67%-20%(1, 2 and 3 ring defects out of 15 at the interface) I_{ON} ranges from 277-293 A(Fig 4(a)-(b)).

Conclusion

From the above analysis, we see that the band gap, effective mass and device characteristics illustrate a minimal change when the defect is mono or divacancy, but the change is more considerable for ring vacancy.

References

[1] Lijie Ci et.al, , Nature Materials **9**, 430 (2010).
[2] A. Chanana et.al, , J. Appl. Phys **115**, 034501 (2014).
[3] J. M. Pruneda , Phys. Rev. B **85**, 045422 (2012).
[4] ATK 13.8, `http://www.quantumwise.com/`

ISBN 978-0-692-50554-0

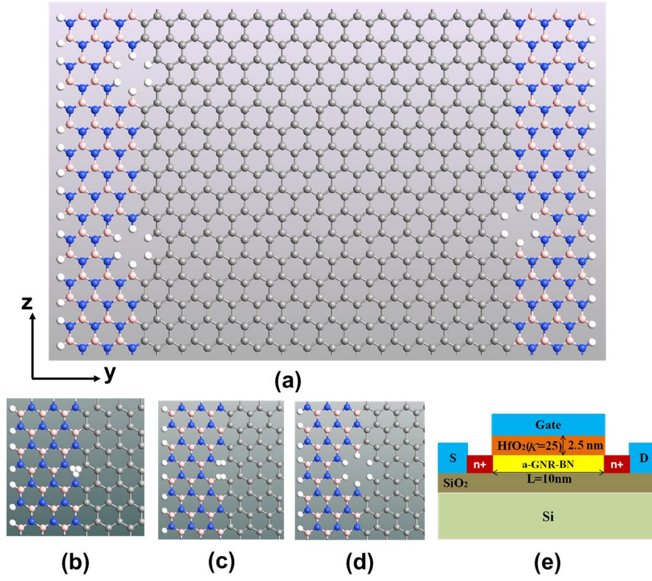

Fig. 1. (a) Supercell used in the present study. It is formed by repeating 8 times the unit cell 42 a-GNRBN. (b),(c) and (d) showing mono vacancy, di vacancy and ring defects all formed at the interface. Hydrogen passivation is done to minimize contribution from edge states (e) Transistor schematic used for the device calculations.

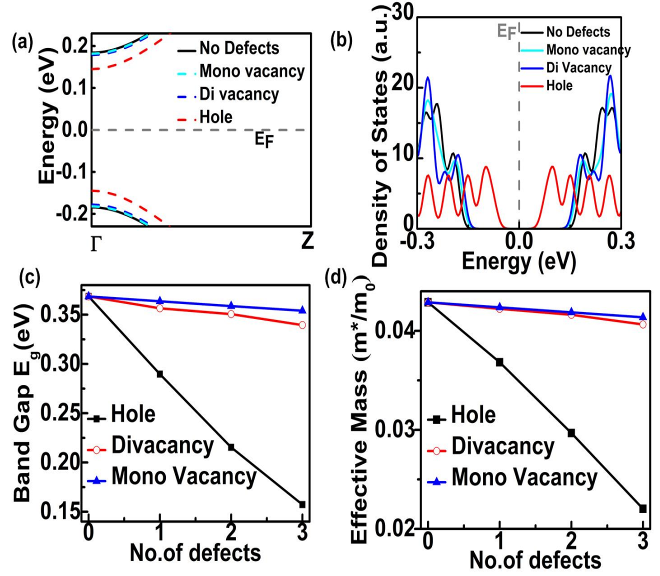

Fig. 2. (a)-(b) Comparison of band structures and density of states of pure and vacancy affected supercell. (c) - (d) Band gap and Effective mass comparison with the increase in number of defects

TABLE I

BANDGAP AND EFFECTIVE MASS OF PURE AND VACANCY AFFECTED SUPERCELL EVALUATED USING DFT (NUMBER OF DEFECT IS 3 FOR EACH TYPE OF VACANCY)

Type of Vacancy defect	Band Gap (eV)	Effective Mass (m^*/m_0)
Pure	0.369	0.0429
Mono vacancy	0.354	0.0413
Di vacancy	0.339	0.0407
Ring vacancy	0.157	0.022

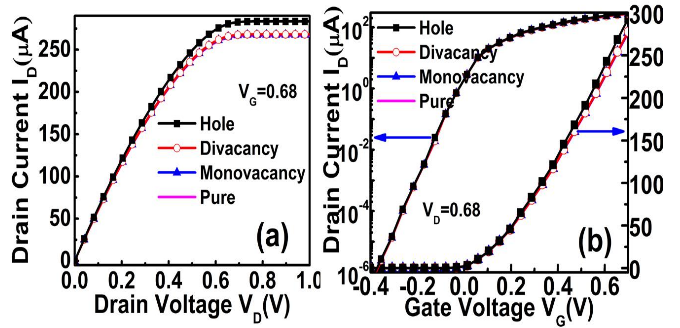

Fig. 3. (a) I_D-V_D and (b) I_D-V_G characteristics of pure and defected supercell. Defect density for each type of vacancy is 3.

TABLE II

N-MOSFET DEVICE PARAMETERS OF PURE AND VACANCY AFFECTED SUPERCELL CALCULATED USING NEGF FORMALISM (NO. OF DEFECT IS 3 FOR EACH TYPE OF VACANCY)

Type of Vacancy defect	$I_{ON}(\mu A)$	Subthreshold Slope (mV/decade)
Pure	98.14	62.096
Mono vacancy	98.38	62.138
Di vacancy	98.5	62.189
Ring vacancy	101.6	62.622

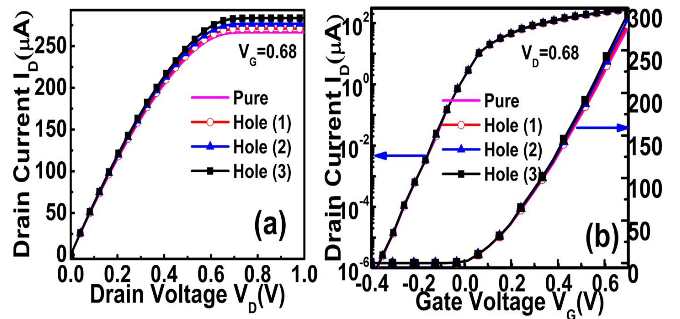

Fig. 4. (a) I_D-V_D and (b) I_D-V_G characteristics ring defects increasing from 1 to 3.